Molecular Crystals and Liquid Crystals

Publication details, including instructions for authors and subscription information:
http://www.tandfonline.com/loi/gmcl16

Negative Endor Study of the Collective Motion in TGS

Ichiro Miyagawa [a] & Yashige Kotake [a]

[a] Department of Physics and Astronomy, The University of Alabama, P.O. Box 1921, Alabama, 35486, U.S.A.

Version of record first published: 21 Mar 2007.

To cite this article: Ichiro Miyagawa & Yashige Kotake (1979): Negative Endor Study of the Collective Motion in TGS, Molecular Crystals and Liquid Crystals, 50:1, 111-125

To link to this article: http://dx.doi.org/10.1080/15421407908084420

Mol. Cryst. Liq. Cryst., 1979, Vol. 50, pp. 111–126

Printed in Holland

Negative Endor Study of the Collective Motion in TGS†

ICHIRO MIYAGAWA and YASHIGE KOTAKE

Department of Physics and Astronomy, P.O. Box 1921, The University of Alabama, University, Alabama 35486, U.S.A.

(*Received June 16, 1978*)

An x-ray irradiated crystal of deuterated triglycine sulphate (DTGS) was studied with the use of negative ENDOR technique. When observed below T_c = 332°K, the signal was found to split into a doublet. It was also found that the intensities of the doublet components were practically equal over the temperature range from 332°K to 175°K. Below 175°K, however, one of the components was found to be weak and broad compared with the other component. These results further supported the collective tunneling model which was proposed in a previous paper.

INTRODUCTION

Hydrogen-bonded ferroelectric crystals have been studied extensively by using various techniques including the neutron diffraction method.[1–3] Especially, triglycine sulphate (TGS) has attracted the interest of many workers because of its ferroelectricity at room temperature[4] and a possible application as excellent infrared detectors.[5] The reported work on TGS include several magnetic resonance studies: deuteron NMR of deuterated crystals,[6–8] nitrogen NMR of a crystal grown from an aqueous solution,[9] electron-nuclear-double-resonance (ENDOR) of irradiated crystals,[10–13] and electron spin resonance (ESR) of doped crystals.[14,15]

An important fact which these magnetic resonance studies have established is that the signal splits into a doublet when the crystal is cooled through the Curie temperature (T_C = 332°K). Moreover, as the temperature decreases, the doublet splitting increases, starting from zero at T_C and approaching a constant value for low temperatures. Doublet splitting of this nature has been observed for the signal from a ^{14}N nucleus and from most of the protons

† This work was supported by the National Science Foundation Grant GU 3205 and the Research Grant Committee (The University of Alabama) Grant 931.

of a TGS crystal. It is true that no such doublet splitting occurs for the signal from the $H_{(7)}$ proton of the O . . . $H_{(7)}$—O between the two glycine molecules GII and GIII[16,17] because of the crystal symmetry.[12] It was shown, however, that in an irradiated crystal this symmetry is destroyed and as a result the signal from $H_{(7)}$ splits into a doublet below T_C.

An unusual fact of the doublet splitting described above is that no evidence for signal broadening has been detected in spite of its strong temperature dependence. Thus, this temperature dependence cannot be explained by an ordinary Brownian tumbling model which accounts for most cases of the temperature dependence for signal splitting in magnetic resonance.[18–21] It has been shown that a simple tunneling model which is called collective tunneling model in the present paper, explains satisfactorily the observed result for doublet splitting.[12]

The above-mentioned doublet splitting shows another interesting fact which has not been explained. In the case of $H_{(7)}$ and the protons with larger hyperfine splitting (hfs), it has been found that the intensities of the doublet components are unequal.[11,12] For the protons with smaller hfs, however, the intensities appear equal between the doublet components. It is noted that the collective tunneling model predicts that all the protons in TGS behave in the same fashion. Thus, the above-mentioned difference in doublet intensities between the two types of protons can possibly be a difficulty of the model. It should be pointed out, however, that in the case of the protons with the smaller hfs, the adjacent signals overlap with each other at low temperatures [see, for example, Figure 4 of ref. 12, especially for signals H_{C_1} and H_N]. Thus, no accurate knowledge may be obtained for the intensity ratio of the doublet components in the case of H_{C_1} and H_N, that is, protons with the smaller hfs. It is expected, however, that in deuterated triglycine sulphate (DTGS), one detects in this frequency range only the H_{C_1} signal from a C—H proton, and the H_N and H_O signals, which arise from an N—H proton and an O—H proton, respectively, disappear [the H_O signal has been assigned to the $H_{(7)}$ proton[12]]. Thus, the absence of signal overlap should allow one to obtain an accurate knowledge on the intensity behavior of the H_{C_1} doublet. For this reason, an ENDOR experiment with DTGS was conducted in the present investigation, and the obtained result was interpreted on the basis of the collective tunneling model.

EXPERIMENTAL

A sample of TGS powder was dissolved into heavy water and recovered by evaporating the solvent under vacuum. Repeating this process three times, the O—H and N—H_2 hydrogens were replaced by deuterium. The resulting DTGS powder was used to prepare a saturated heavy water solution. Single

crystals of DTGS were grown from this solution with the use of a slow cooling technique.

The crystal of DTGS was irradiated for 1.5 hours at room temperature in an x-ray source operating at 40 kV and 30 mA. The irradiated crystal was annealed for two days in order to quench the unstable radical.[22]

The ENDOR spectrometer employed is described in a previous paper.[23] It should be mentioned that the ENDOR signals in the presently employed spectrometer arise from a reduction of the ESR signals by intense radio-frequency field, rather than an enhancement. Because of this "negative enhancement" we call this technique negative ENDOR. A negative ENDOR signal is stronger than the corresponding conventional ENDOR signal by a factor of ten or more for most proton signals. Negative ENDOR technique has already been applied to several irradiated crystals.[12,13,24,25] Recently two detection modes of negative ENDOR were discovered: in-phase and out-of-phase.[26] The out-of-phase mode was used in the present investigation because of a better signal-to-noise ratio in the covered frequency range, 11–13 MHz. The employed radio-frequency field was 7 G, which was measured with the use of the sideband technique.[27]

The negative ENDOR signals were observed over a temperature range from 135°K to 370°K. A copper-constantan thermocouple was used to measure the temperature of the sample crystal.

In all the observations, the magnetic field was applied parallel to the ferroelectric *b*-axis, so that there was no site splitting to complicate the spectrum.

EXPERIMENTAL RESULT

Figure 1 shows the negative ENDOR signals from the H_{C_1} proton. The top curve was taken at 366°K which is above T_C = 322°K, and the bottom two curves were taken at temperatures below T_C. As was expected, the signal did not overlap with the signals from the other protons.

Figure 2 compares the temperature dependence of the H_{C_1} doublet splitting for DTGS with that for TGS. Note that both splittings decrease to zero at the corresponding Curie temperatures, respectively.

Figure 3 shows the ENDOR signals for DTGS and TGS in the neighborhoods of their Curie temperatures. The splitting for DTGS increases with decreasing temperature much faster than that for TGS. It is noted, however, that for DTGS no significant change in line width was detected in spite of this fast increase in splitting. This result further confirmed that the temperature dependence of the doublet splitting is not associated with an ordinary Brownian tumbling.

The absence of overlap in signal for DTGS allows one to measure the intensities of the doublet components accurately. Figure 4 plots the ratio of

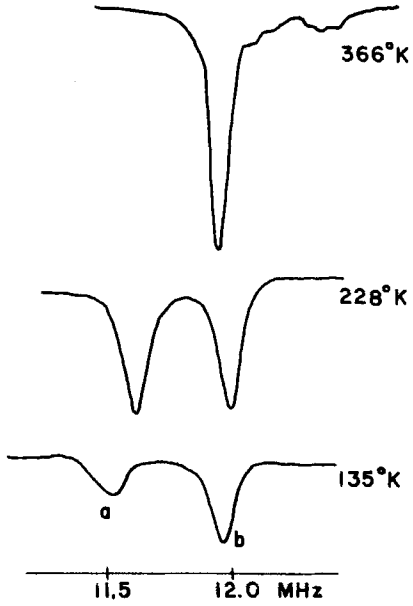

FIGURE 1 ENDOR signal from the H_{C_1} proton. The signal splits into a doublet when $T < T_C = 332°K$.

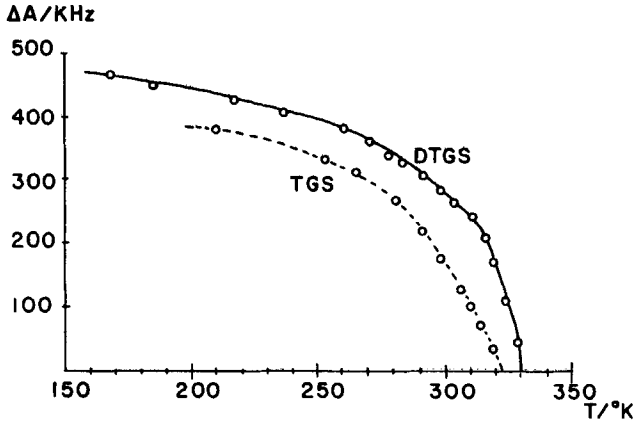

FIGURE 2 Temperature dependence of the doublet splitting ΔA for H_{C_1}. The dotted curve represents the case of TGS.

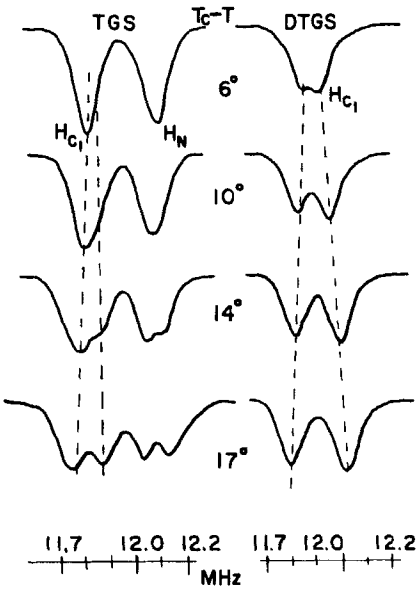

FIGURE 3 Doublet splitting near T_c in the ferroelectric phase.

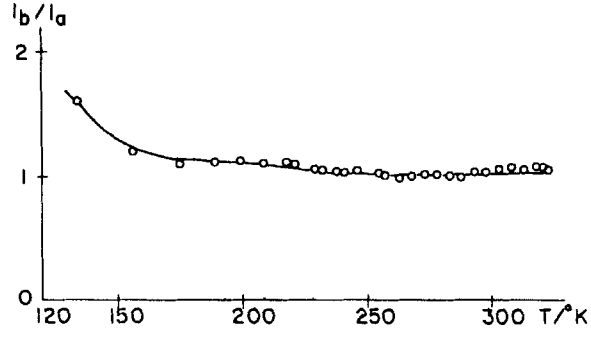

FIGURE 4 Plots of the intensity ratio of the doublet components from H_{c_1} against temperature. The integrated intensity is used to obtain the ratio.

the integrated intensities against temperature. One notices that if the result below 170°K is disregarded, the ratio is practically equal to 1.00: The average value is 1.05 with the deviation less than 0.07. Below 170°K, the line width of peak *a* increased substantially with decreasing temperature while that of peak *b* increased only by a small amount. As the bottom figure of Figure 1 shows, at 135°K the line width of peak *a* is broader than that of peak *b* by 70%.

DISCUSSION

The presently observed result clarified some detail of the collective tunneling model, which is called simple tunneling model in a previous paper.[12] This model is an extension of Blinc's tunneling model,[28] which was applied to explain the isotope effect in ferroelectric transition temperature. It is noted, however, that for interpretation of the doublet splitting, Blinc's group uses a special Brownian tumbling model,[9,29] which is known as the dynamical order–disorder model.

1) Collective Tunneling Model. The assumption for this model should be improved in clarity. It is assumed that a ferroelectric domain consists of many regions, each region containing many molecules; all the molecules in each region tunnel collectively and hence coherently; the collective tunnelings in different regions are incoherent; the tunneling motion of each molecule is a combination of vibrational, rotational and deformational tunnelings; the effective tunneling potential for each molecule is a double-minimum one with unequal energies [see Fig. 5]; the energy difference ΔE° is identical for every molecule in the crystal, and so is the effective exchange integral Γ.

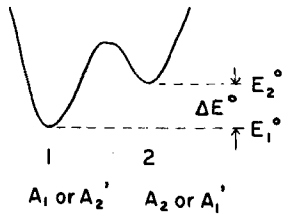

FIGURE 5 Double-minimum potential.

Consider a nucleus which has wave functions ϕ_1 and ϕ_2 at the two energy minima, respectively. The eigenvalue is given by

$$E_\pm = \mp[(\Delta E^\circ/2)^2 + \Gamma^2]^{1/2} + (E_1^\circ + E_2^\circ)/2. \tag{1}$$

The corresponding eigenfunctions are

$$\Phi_+ = C_1\phi_1 + C_2\phi_2, \tag{2}$$

$$\Phi_- = C_2\phi_1 - C_1\phi_2, \tag{3}$$

where

$$C_1 = [(\Delta E + \Delta E^\circ)/(2\Delta E)]^{1/2}, \tag{4}$$

$$C_2 = [(\Delta E - \Delta E^\circ)/(2\Delta E)]^{1/2}, \tag{5}$$

$$\Delta E = E_- - E_+ = [(\Delta E^\circ)^2 + 4\Gamma^2]^{1/2}. \tag{6}$$

The hyperfine splitting (hfs) tensor may be computed with the use of the eigenfunctions Φ_+ and Φ_-. Since the hfs interaction $\mathscr{H}_{\text{hfs}}$ is much weaker than the exchange interaction resulting in Γ, one obtains

$$(\Phi_1 | \mathscr{H}_{\text{hfs}} | \Phi_1) = A_1, \tag{7}$$

$$(\Phi_2 | \mathscr{H}_{\text{hfs}} | \Phi_2) = A_2, \tag{8}$$

where A_1 and A_2 are the z-components of the hfs tensor at the two potential minima, respectively, that is, the components parallel to the applied field. Furthermore, one may assume for simplicity

$$(\Phi_1 | \mathscr{H}_{\text{hfs}} | \Phi_2) = (\Phi_2 | \mathscr{H}_{\text{hfs}} | \Phi_1) = 0. \tag{9}$$

Consequently, the z-components of the hfs tensor for the two eigenstates are given by

$$A_+ = (\Phi_+ | \mathscr{H}_{\text{hfs}} | \Phi_+) = C_1^2 A_1 + C_2^2 A_2, \tag{10}$$

$$A_- = (\Phi_- | \mathscr{H}_{\text{hfs}} | \Phi_-) = C_2^2 A_1 + C_1^2 A_2. \tag{11}$$

Thus, the nucleus produces two signals, the components of which appear at the frequencies corresponding to A_+ and A_-, respectively, with the intensity ratio $1 : \exp(-\Delta E/kT)$. From the preceding equations, one obtains the difference between the two frequencies ΔA

$$\Delta A/(A_1 - A_2) = [1 + (2\Gamma/\Delta E^\circ)^2]^{-1/2}. \tag{12}$$

It is evident that the preceding treatment applies without fundamental modification to other cases of doublet splitting including that in deuteron NMR.

2) Model for the Phase Transition. Three models have been proposed for the phase transition of TGS; displacive model,[8] dynamical order–disorder model,[7,9] and collective tunneling model.[12] The second two are dynamical models. The second model will be called collective jumping model in this paper. In this section, the assumption for these models will be discussed and will be improved in clarity, if necessary.

First, the accepted model for polarization reversal will be described.[16,17] In the ferroelectric phase, there are three different pairs of glycine molecules in a unit cell, which are designated as GI, GII and GIII.[16,17] Chemically GII is a zwitter ion ($NH_3^+CH_2CO_2^-$), while GI and GIII are glycinium ions ($NH_3^+CH_2COOH$). Moreover, GII and GIII form a pair, which is written by

$$\underset{\text{GII}}{\overset{\overset{O}{\|}}{NH_3^+CH_2C-O^-}} \cdots \underset{(7)}{H} \underset{\text{GIII}}{\overset{\overset{O}{\|}}{-O-CH_2CNH_3^+}}. \tag{13}$$

When the $H_{(7)}$ proton shifts from right to left, the resulting structure of the pair will be

$$\underset{\text{GIII}}{\overset{\overset{O}{\|}}{NH_3^+CH_2C}}—O—H_{(7)}\cdots O^-—\underset{\text{GII}}{\overset{\overset{O}{\|}}{CH_2CNH_3^+}}. \qquad (14)$$

Thus, the glycine molecules convert in structure as

$$\text{GII} \rightarrow \text{GIII};\ \text{GIII} \rightarrow \text{GII}. \qquad (15)$$

When this conversion occurs, the remaining glycine molecule GI changes its orientation cooperatively. Hence, the dipole moment of GI changes its orientation cooperatively. This series of cooperative molecular motions leads to the conversion from the crystal structure in one ferroelectric domain to the structure in the other domain.

The crystal structure in one domain is the mirror image of the structure in the other domain with regard to planes (0, 1/4, 0) and (0, 3/4, 0) which are perpendicular to the ferroelectric *b*-axis [see Figure 6]. It is also noted that because of the screw axis 2_1, the crystal structures in the two different domains are related by inversion operation at points [0, 0, 0] and [0, 1/2, 0], which are indicated by the dotted circles. For this reason, all the physical properties of a ferroelectric TGS crystal must conform with these mirror symmetry

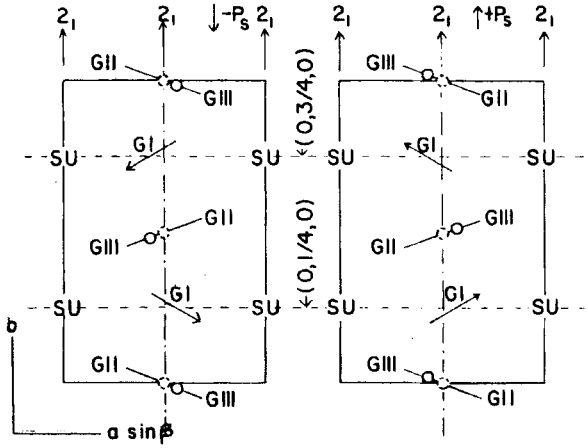

FIGURE 6 Schematic crystal structure below T_c based on crystal analysis studies.[16,17] The projection perpendicular to the c-axis is shown in the case of both domains with positive and negative polarization P_s. The circle indicates $H_{(7)}$; GII is a zwitterion ($NH_3^+CH_2CO_2^-$); GI and GIII with $H_{(7)}$ are glycinium ions ($NH_3^+CH_2COOH$); SU is a sulphate ion. The arrow under GI indicates the dipole moment of GI schematically. The screw axis is denoted by 2_1. The point which is indicated by the broken circle becomes an inversion point when $T > T_c$. Planes (0, 1/4, 0) and (0, 3/4, 0) become mirror planes when $T > T_c$.

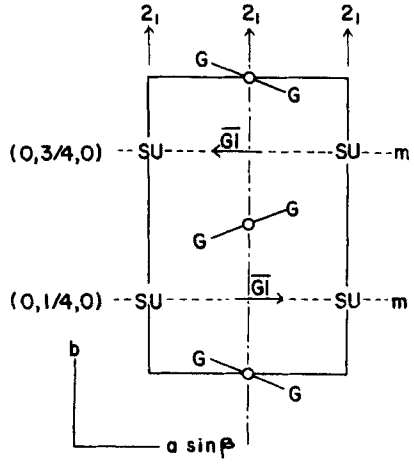

FIGURE 7 Schematic crystal structure similar to the one in Figure 6 but above T_C. Note that $H_{(7)}$ is on the inversion point, and the dipole moment of $\overline{GI}$ is parallel to the mirror plane.

and inversion symmetry operations. Thus, the spontaneous polarization P_s must be parallel to the b-axis in one domain, and antiparallel in the other domain. Consequently, the above-mentioned series of cooperative motions results in inversion of P_s. This is the accepted model of the polarization reversal in TGS. It should be mentioned that P_s predominantly arises from the dipole moment of GI, which is denoted by the arrow under GI in Figure 6. The circle on GII–GIII indicates $H_{(7)}$.

When $T > T_C$ [see Figure 7], a TGS crystal has the real mirror symmetry with regard to planes (0, 1/4, 0) and (0, 3/4, 0) and the real inversion symmetry with regard to points [0, 0, 0] and [0, 1/2, 0]. Thus, all the physical properties of the crystal must conform with these mirror and inversion symmetries. As a result, P_s must be zero. Consequently above T_C the crystal is not ferroelectric but paraelectric. It is noted that because of the symmetries, there is no difference between GII and GIII, whose notations are now replaced by G. It is also noted that the $H_{(7)}$ proton is now on the inversion point; the dipole moment of GI, which is now denoted by $\overline{GI}$, is parallel to the symmetry plane.

In the displacive model of phase transition, it is assumed that the crystal structure of each domain gradually approaches the one in the paraelectric phase with increasing temperature, converting to the latter completely at T_C.

The dynamical models are rather complex. The basic assumption, which will later be refined to some extent, is as follows: (i) At a given temperature, structure GII is given by a dynamical average of two structures GII° and

GIII°, where GII° and GIII° are identical with GII and GIII at 0°K, respectively; (ii) a rapid switching occurs between GII° and GIII°

$$\text{GII}^\circ \rightleftarrows \text{GIII}^\circ; \tag{16}$$

(iii) this switching in structure results from a switching of every nucleus in the molecule between two positions, that is, one in GII° and the other in GIII°; (iv) these two positions are represented by the two minima in a double-minimum potential, respectively [see Figure 5]; (v) every nucleus of the molecule has the same value of ΔE°; (vi) structure GIII at a given temperature is given by a similar dynamical average; (vii) structure GI at a given temperature is given by a similar dynamical average but of two structures GI^0_+ and GI^0_-, where GI^0_+ is identical with GI in the positive P_s phase at 0°K, and GI^0_- with GI in the negative P_s phase at 0°K.

It is evident that the symmetry property of the crystal requires: assumption (vii) leads to that GI^0_+ and GI^0_- are related by a reflection with regard to plane (0, 1/4, 0) or plane (0, 3/4, 0). In addition, the same assumption requires that a rapid switching occurs between GI^0_+ and GI^0_-

$$\text{GI}^0_+ \rightleftarrows \text{GI}^0_-. \tag{17}$$

The collective nature of the dynamical models requires further assumptions: (viii) the switching given by Eq. (16) in structure GII, a similar switching in structure GIII, and the switching given by Eq. (17) in structure GI take place synchronously. This requires that (ix) the same value of ΔE° is taken for the effective double-minimum potential for every nucleus in these three molecules; (x) every nucleus in these three types of molecules in a given region, which is assumed in the preceding section, switches synchronously between the two minima in the effective double-minimum potential.

Because of the crystal structure and the collective nature, ΔE° arises predominantly from the interaction between the dipole moment of GI and the electric field originating from P_s.

Finally, the two dynamical models differ from each other by the assumption: (xi) in the collective jumping model, the switching between the two minima is a classical Brownian jumping; in the collective tunneling model, the switching is a quantum tunneling. The mathematical detail of the tunneling was already given in the preceding section.

Some refinement should be made for assumptions (i) and (vii). This refinement is important for explaining the spectra at low temperatures, as will be shown. For example, it was assumed in (i) that structure GII° was identical in both lower and higher energy minima. This assumption is probably correct, if the temperature is not very low, and hence ΔE° is relatively small. At very low temperatures, ΔE° should be large because of large P_s. Hence, the structure should be deformed by an interaction energy of $-\Delta E^\circ/2$ in the lower

minimum and $+\Delta E^\circ/2$ in the higher minimum. Consequently, the temperature-independent structure GII° should be replaced by a slightly temperature-dependent structure GII_1 for the lower minimum and by GII_2 for the higher minimum. A similar discussion should apply to GIII°. Thus, Eq. (16) should be replaced by

$$GII_1 \rightleftarrows GIII_2; GIII_1 \rightleftarrows GII_2, \tag{18}$$

and Eq. (17) by

$$GI_{+1} \rightleftarrows GI_{-2}; GI_{-1} \rightleftarrows GI_{+2}, \tag{19}$$

the former being for the positive phase and the latter being for the negative phase. It is noted that GI_{+1} is equivalent with GI_{-1}, and GI_{+2} with GI_{-2}.

In the paraelectric phase, $P_s = 0$ and hence $\Delta E^\circ = 0$. Thus in both models,

$$GII_1 = GII_2 = GII^\circ; GIII_1 = GIII_2 = GIII^\circ.$$

Consequently, the dynamical average is given by

$$G = (GI^\circ + GII^\circ)/2,$$

for both GII and GIII. Similarly

$$GI_{+1} = GI_{+2} = GI_+^0; GI_{-1} = GI_{-2} = GI_-^0,$$

and hence the dynamical average is given by

$$GI = (GI_+^0 + GI_-^0)/2.$$

Thus, the resulting structure, which will be the one shown in Figure 7, has the mirror symmetry. Hence, P_s will be zero, as is required for the paraelectric phase. Consequently in both dynamical models, the phase transition occurs as follows: As the temperature increases, P_s and hence ΔE° decreases; as a result, the structure for each domain, which is given as a dynamical average, approaches the structure for the paraelectric phase; eventually at T_C the former completely converts to the latter.

3) Doublet Splitting. When the switching given by Eq. (18) occurs, a proton in GII_1 switches to the corresponding proton in $GIII_2$. In the double-minimum potential in Figure 5, this proton motion is a switching from minimum 1 to minimum 2. Hence the magnetic resonance frequency switches from A_1 to A_2. Equation (18) also indicates that a proton in $GIII_1$ switches to the corresponding proton in GII_2. When $T > T_C$, this proton is equivalent with the proton in the first switching. In Figure 5, this proton switches from minimum 1 to minimum 2 because of the collective nature of switching. The frequency switches, however, from A_2' to A_1' [see Figure 5]. Thus, the

switching in frequency is given by

$$A_1 \rightleftarrows A_2; A_2' \rightleftarrows A_1'. \tag{20}$$

It is noted that when $T > T_C$, $A_1 = A_1'$ and $A_2 = A_2'$ since $GII_1 = GII_2 = GII^\circ$ and $GIII_1 = GIII_2 = GIII^\circ$. When $T < T_C$ in general $A_1 \neq A_1'$ and $A_2 \neq A_2'$, since $GII_1 \neq GII_2$ and $GIII_1 \neq GIII_2$. If the temperature is not very low, however, one may assume that

$$A_1 \simeq A_1'; A_2 \simeq A_2', \tag{21}$$

since the electrostatic deformation of molecules should be small.

In the collective tunneling model, the first switching in Eq. (20) results in signals at A_+ and A_- [see Eqs. (14) and (15)]. The intensity ratio of the two signals is 1; $\exp[-\Delta E/kT]$, where ΔE is the energy difference between the Φ_+ and Φ_- states. The expected spectrum is shown in Figure 8(a).

If the temperature is not very low, the second in Eq. (20) results in two signals which are practically identical with the preceding signals because of Eq. (21). It is noted, however, that the intensity ratio is now $\exp[-\Delta E/kT]:1$. That is, the intensity relation of the doublet components is opposite to that in the preceding case. The resulting spectrum is given in Figure 8(b).

The spectrum expected for the tunneling given by Eq. (20) is the sum of the two spectra in (a) and (b). Figure 8(c) shows this spectrum which is a doublet of equal components.

The above doublet is expected for an unirradiated crystal of TGS. In an irradiated crystal, GII and GIII are expected to turn to radicals with equal

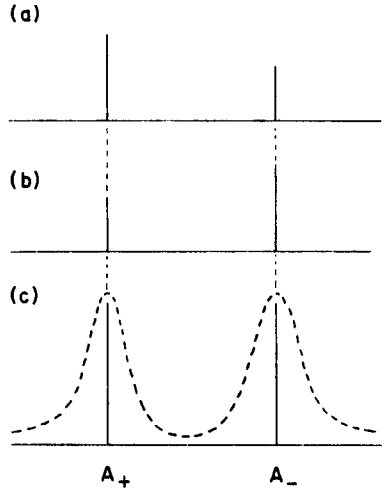

FIGURE 8 ENDOR doublet spectrum arising from tunneling at a moderate temperature below T_C. The spectrum in (c) is the sum of the spectra in (a) and (b).

probabilities. Thus in a given domain, if GIII is a radical, the signal frequency is in the ENDOR range for the protons of GII and in the higher ESR range for the protons of GIII. Hence in this case, the resulting ENDOR signal is the one shown in Figure 8(a). For a similar reason, when GII is a radical, the resulting ENDOR signal is the one shown in Figure 8(b). Thus, the expected signal is again the doublet shown in Figure 8(c). This is the spectrum observed above 170°K. Note that Eq. (12) predicts that the doublet separation ΔA decreases with decreasing ΔE° which decreases with increasing temperature. Thus for $T \geq T_C$, no doublet splitting is expected because of $\Delta E^\circ = 0$. This prediction is in agreement with observation.

When the temperature is very low, the difference between A_1 and A_1' and that between A_2 and A_2' could no longer be disregarded. If for a special case, A_- is fairly close to A_-', the expected spectrum would be the one shown in Figure 9(c). Note that the signal component at the lower frequency is broad while the one at the higher frequency is relatively sharp. This is the spectrum observed below 170°K down to 135°K [see the spectrum for 135°K in Figure 1].

It should be pointed out that the intensity of a negative ENDOR signal is sensitive to line width.[23] Thus, when a signal is broad, the integrated intensity as well as the peak intensity appear weak.

In the case of H_O and protons with larger hfs, the difference between A_1 and A_1' and that between A_2 and A_2' would be fairly large because of relatively large values of A's even at fairly high temperatures. Thus, the intensities of the doublet components would appear unequal even at high temperatures in the ferroelectric range. This was found to be the case.

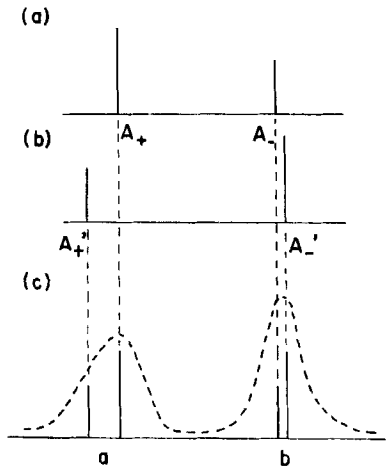

FIGURE 9 Spectrum similar to the one in Figure 8 but for a low temperature.

In conclusion, it was shown in the present investigation that the collective tunneling model explains at least semi-quantitatively the relative intensities of the doublet components for the observed proton ENDOR signals over the range from 135°K to 370°K.

In the previous paper,[12] it has been attempted to deduce the value of Γ from the temperature dependence of the intensity ratio of the doublet components for H_0, that is $H_{(7)}$. Such an estimation is not possible since the intensity difference of the components does not arise from ΔE but rather from the difference in the A values.

It should be noted that the ENDOR experiment is sensitive to the damage center rather than undamaged molecules in an irradiated crystal. The previous investigation[13] has shown, however, that the ENDOR doublet represents essentially a property of an unirradiated ferroelectric crystal, although a minor correction for radiation effect is needed. Moreover, it is noted that this correction is required for the doublet separation; no such correction is needed for the intensity ratio of the doublet components.

CONCLUDING REMARKS

It is of interest to note that neither the displacive model nor the collective jumping model predicts the low temperature spectrum shown at the bottom in Figure 1. In the displacive model, the doublet components should appear at the two frequencies corresponding to GII and GIII. Especially, the intensities are expected to be equal over the whole range of ferroelectricity. This disagrees with the spectrum observed below 170°K. It should be pointed out that several facts unfavorable for the displacive model have already been known. These facts include: a relatively large value for the transition entropy (0.48 cal/mol. deg.),[30] a relatively small value of the Curie–Weiss constant (3280°K),[31] the result of the critical x-ray scattering,[31] and the average value for doublet components of ^{14}N quadrupole interaction for GI.[9]

The collective jumping model assumes a jumping between the two minima of a double-minimum potential with a rate much faster than the doublet splitting. Hence the model predicts a temperature-dependent doublet splitting without broadening. The frequencies of the doublet components should be given by

$$[A_1 + A_2 \exp(-\Delta E^\circ/kT)]/[1 + \exp(-\Delta E^\circ/kT)];$$
$$[A_2' + A_1' \exp(-\Delta E^\circ/kT)]/[1 + \exp(-\Delta E^\circ/kT)]. \qquad (22)$$

Thus, the model is successful above 170°K. However, this model fails below 170°K, because no broadening is expected.

In view of the preceding discussion, the doublet observed below 170°K appears to support the collective tunneling model rather than the displacive model and the collective jumping model. If the collective tunneling model is really the correct one, the predicted spectrum in Figure 9(c) has to be observed. In particular, the splitting of each doublet components has to be resolved. For this reason, it is desired that the observation temperature be further lowered. This experiment requires a further improvement of the sensitivity of the spectrometer, since the signal below 135°K is very weak.

The Fujimoto–Dressel model,[15] which is fundamentally different from the three models described, was not considered in the present paper, since this model is intended to apply to the case of a dipolar impurity.

References

1. R. Blinc and B. Zeks, "Soft Modes in Ferroelectrics and Antiferroelectrics," North-Holland, Amsterdam, 1974.
2. J. L. Bjorkstam, *Advan. Magn. Reson.*, **7**, 1 (1974).
3. G. Bacon and R. Pease, *Proc. Roy. Soc. Ser. A*, **220**, 397 (1953); **230**, 359 (1955).
4. F. Jona and G. Shirane, "Ferroelectric Crystals," Pergamon, Oxford, 1962.
5. K. L. Bye, P. W. Whipps and E. T. Keve, *Ferroelectrics*, **4**, 253 (1972).
6. R. Blinc, S. Detoni and M. Pintar, *Phys. Rev.*, **124**, 1036 (1961).
7. R. Blinc, M. Pintar and I. Zupančič, *J. Phys. Chem. Solids*, **28**, 405 (1967).
8. J. L. Bjorkstam, *Phys. Rev.*, **153**, 599 (1967).
9. R. Blinc, M. Mali, R. Osredkar, A. Prelesnik, I. Zupančič and E. Ehrenberg, *J. Chem. Phys.*, **55**, 4843 (1971); *Acta Chem. Scand.*, **25**, 2403 (1971).
10. M. Welter and W. Windsch, *Proc. Colloq. AMPÉRE*, **16**, 435 (1970).
11. W. Windsch, M. Welter and W. Driesel, *Ferroelectrics*, **8**, 551 (1974).
12. Y. Kotake and I. Miyagawa, *J. Chem. Phys.*, **64**, 3169 (1976).
13. J. L. Yeh and I. Miyagawa, *J. Phys. Chem. Solids*, **38**, 1371 (1977).
14. T. Kato and R. Abe, *J. Phys. Soc. Japan*, **36**, 1065 (1974).
15. M. Fujimoto and L. A. Dressel, *Ferroelectrics*, **8**, 611 (1974).
16. S. Hoshino, Y. Okaya and R. Pepinski, *Phys. Rev.*, **115**, 323 (1959).
17. M. I. Kay and R. Kleinberg, *Ferroelectrics*, **5**, 45 (1973).
18. I. Miyagawa and K. Itoh, *J. Chem. Phys.*, **40**, 2157 (1962).
19. T. Chiba, *J. Chem. Phys.*, **39**, 947 (1963).
20. C. S. Johnson, Jr., *Advan. Magn. Reson.*, **1**, 33 (1965).
21. P. D. Sullivan and J. P. Bolton, *Advan. Magn. Reson.*, **4**, 39 (1970).
22. T. Kato, R. Abe and I. Suzuki, *J. Phys. Soc. Japan, Suppl.*, **28**, 123 (1970).
23. I. Miyagawa, R. B. Davidson, H. A. Helms, Jr. and B. A. Wilkinson, Jr., *J. Magn. Reson.*, **10**, 156 (1973).
24. H. A. Helms, Jr., I. Suzuki and I. Miyagawa, *J. Chem. Phys.*, **59**, 5055 (1973).
25. I. Suzuki, *J. Phys. Soc. Japan*, **37**, 1379 (1974).
26. Y. Hayashi and I. Miyagawa, *J. Magn. Reson.*, **28**, 351 (1977).
27. I. Miyagawa, Y. Hayashi and Y. Kotake, *J. Magn. Reson.*, **25**, 183 (1977).
28. R. Blinc, *J. Chem. Phys. Solids*, **13**, 204 (1960).
29. R. Blinc, *Advan. Magn. Reson.*, **3**, 141 (1963).
30. S. Hoshino, T. Mitsui, F. Jona and R. Pepinsky, *Phys. Rev.*, **107**, 1255 (1957).
31. I. Shibuya and T. Mitsui, *J. Phys. Soc. Japan*, **16**, 479 (1961).